

## Hierarchical Optimal Maneuver Planning and Trajectory Control at On-Ramps With Multiple Mainstream Lanes

Chen, Na; van Arem, Bart; Wang, Meng

**DOI**

[10.1109/TITS.2022.3167727](https://doi.org/10.1109/TITS.2022.3167727)

**Publication date**

2022

**Document Version**

Final published version

**Published in**

IEEE Transactions on Intelligent Transportation Systems

**Citation (APA)**

Chen, N., van Arem, B., & Wang, M. (2022). Hierarchical Optimal Maneuver Planning and Trajectory Control at On-Ramps With Multiple Mainstream Lanes. *IEEE Transactions on Intelligent Transportation Systems*, 23(10), 18889-18902. <https://doi.org/10.1109/TITS.2022.3167727>

**Important note**

To cite this publication, please use the final published version (if applicable).  
Please check the document version above.

**Copyright**

Other than for strictly personal use, it is not permitted to download, forward or distribute the text or part of it, without the consent of the author(s) and/or copyright holder(s), unless the work is under an open content license such as Creative Commons.

**Takedown policy**

Please contact us and provide details if you believe this document breaches copyrights.  
We will remove access to the work immediately and investigate your claim.

***Green Open Access added to TU Delft Institutional Repository***

***'You share, we take care!' - Taverne project***

**<https://www.openaccess.nl/en/you-share-we-take-care>**

Otherwise as indicated in the copyright section: the publisher is the copyright holder of this work and the author uses the Dutch legislation to make this work public.

# Hierarchical Optimal Maneuver Planning and Trajectory Control at On-Ramps With Multiple Mainstream Lanes

Na Chen<sup>ID</sup>, Bart van Arem<sup>ID</sup>, *Senior Member, IEEE*, and Meng Wang<sup>ID</sup>, *Member, IEEE*

**Abstract**—Connected Automated Vehicles (CAVs) have the potential to improve traffic operations when they cooperatively maneuver in merging sections. State-of-the-art approaches in cooperative merging either build on heuristics solutions or prohibit mainline CAVs to change lane on multilane highways. This paper proposes a hierarchical cooperative merging control approach that ensures collision-free and traffic-efficient merging through the interaction of a maneuver planner and an operational trajectory controller. The planner predicts future vehicular trajectories, including acceleration trajectories and time instants when lane changes start, in a long horizon up to 50 seconds with a linear prediction model. It establishes the optimal dynamic vehicle sequence in each lane by minimizing predicted traffic disturbances that can propagate upstream and lead to traffic breakdown. During the process, mainline vehicles may change lane to facilitate the on-ramp merging, albeit with a higher ego cost. The operational controller follows the established instructions from the planner and regulates vehicular trajectories with model predictive control in a shorter horizon of 6 seconds. The performance of the designed hierarchical cooperative merging control approach was compared to a cooperative merging method utilizing widely used *first-in-first-out* rule to establish merging sequences and the same operational controller to generate vehicular trajectories. Systematic comparison shows that the proposed approach consistently results in less disturbances during merging under 528 different scenarios with different traffic states, initial vehicular states, and desired time gap settings. On average, a decrease of 39.18% in disturbances was observed.

**Index Terms**—Connected automated vehicles, on-ramp merging, merging sequence, lane-changing decision, multiple lanes.

## NOTATION

$a_i$	Acceleration of vehicle $i$
$a_i^s$	The upper bound of allowed acceleration for CAV $i$
$a^{int}$	vehicle-vehicle interaction acceleration
$a_{\max}$	Maximum acceleration

$a_{\min}$	Maximum deceleration
$D_k$	Models parameters ( $k=1, \dots, 7$ )
$i, j$	Index of CAVs
$l_{veh}$	Vehicle length
$O_{i,j}$	the vehicle sequence between CAV $i$ and $j$ based on all CAVs' lateral and longitudinal positions
$P_{i,j}$	the desired vehicle sequence between CAV $i$ and $j$ according to the planner
$s_0$	Minimum inter-vehicle distance at standstill
$s_i^d$	Desired inter-vehicle gap of CAV $i$
$t_0$	Updated starting time instant of the operational controller
$t_d$	Desired time gap
$t_{\min}^d$	The minimum safe time gap
$\Delta \hat{t}$	Time step used in the planner
$\Delta t$	Time step used in the operational controller
$T$	Control time horizon of the planner
$T_p$	Prediction time horizon of the operational controller
$\mathbf{U}^o$	Control vector of the operational controller
$\mathbf{U}^p$	Control vector of the planner
$v_i$	Speed of vehicle $i$
$v^{\text{limits}}$	Speed limits
$x_e$	Ending position of the acceleration lane
$x_i$	Longitudinal position of vehicle $i$
$y_i$	Lateral position of vehicle $i$
$y_i^t$	Target lateral position of vehicle $i$
$\mathbf{Z}^o$	State vector of the operational controller
$\mathbf{Z}^p$	State vector of the planner
$\xi_i$	Safe lane-changing acceptability of vehicle $i$

## I. INTRODUCTION

THE spatial and temporal dimensions of interactions between mainline and on-ramp traffic on highways trigger congestion, traffic oscillation, and incidents if inter-vehicle spaces are less than desired values [1]. Connected automated vehicles (CAVs) are effective countermeasures to improve traffic operations near on-ramps [1]–[5]. CAVs are equipped with on-board sensors to detect ambient driving environment. Besides, they have communication units and share information among themselves or other entities through Vehicle-to-everything (V2X) communication to enhance situation awareness, thus having high potential to bring benefits in

Manuscript received July 19, 2021; revised February 15, 2022; accepted April 6, 2022. This work was supported in part by the Rijkswaterstaat and in part by the China Scholarship Council. The Associate Editor for this article was J. E. Naranjo. (*Corresponding author: Meng Wang.*)

Na Chen and Bart van Arem are with the Department of Transport and Planning, Delft University of Technology, 2628 CN Delft, The Netherlands (e-mail: DrNaChen@126.com; B.vanArem@tudelft.nl).

Meng Wang is with the Department of Transport and Planning, Delft University of Technology, 2628 CN Delft, The Netherlands, and also with the Friedrich List<sup>†</sup> Faculty of Traffic and Transport Sciences, Technische Universität Dresden, 01069 Dresden, Germany (e-mail: meng.wang@tu-dresden.de).

Digital Object Identifier 10.1109/TITS.2022.3167727

1558-0016 © 2022 IEEE. Personal use is permitted, but republication/redistribution requires IEEE permission.

See <https://www.ieee.org/publications/rights/index.html> for more information.

traffic operations [2], [6]–[11]. The movement of automated vehicles are generally controlled by a maneuver planning and trajectory control and a trajectory following controller [12]–[14]. The maneuver planning and trajectory control controller schedules dynamic vehicle sequences in each lane and plans reference trajectory online or offline in advance. The trajectory following controller commands vehicular actuators to track the planned trajectory as close as possible. In this study, our scope focuses on maneuver planning and trajectory control.

The maneuver planning and trajectory control controller, in general, predicts interaction-aware maneuvers of the surrounding vehicles, schedules a merging sequence, and guides a lane changer to a given slot safely by regulating trajectories of ambient controlled vehicles [15]–[17]. The merging sequence reflects the sequences of vehicles in each lane, thus indicating a vehicle's future directly preceding and following vehicles, respectively. Both merging sequence scheduling and trajectory control impact traffic efficiency or traffic operations.

### A. Literature Review

The policy of complete mainline right-of-way is rarely considered in scheduling dynamic vehicle sequences in each lane for merging efficiency. In [18], 100% mainline right-of-way merging discipline resulted in a reduction of 50%+ from the theoretical maximum capacity. By comparison, making mainline and on-ramp vehicles cooperate to create large enough inter-vehicle distances for on-ramp vehicles to merge at a merging point improved traffic efficiency and only resulted in a reduction of 25%-30% from the maximum capacity. On the other hand, making an on-ramp platoon merge into two consecutive mainline vehicles deteriorate traffic efficiency. In [18], if on-ramp vehicles formed into a platoon before entry and merged as a platoon, the merging process brought a reduction of 40% from the maximum capacity. In [3], letting one on-ramp vehicle merge into mainline traffic was observed to affect the mainline traffic stream less than making an on-ramp platoon merge into the mainline traffic. A review of existing cooperative merging approaches is presented below.

1) *Feasible Trajectory Control*: Initially, motion planning is given more attention. Automated vehicles have a great potential to improve traffic throughput by maintaining small inter-vehicle distances. Regulating automated vehicles to have desired speeds and small inter-vehicle distances before they reach a merging point or the end of the acceleration lane becomes the main research focus in [3], [8], [10], [13], and [19]. A merging sequence, at this stage, can be coupled together with the trajectory or motion planning. In [12], each vehicle was assumed to reach a prescribed merging velocity with constant acceleration. A sequence control layer calculated predicted times-to-go of all vehicles in a control zone to a merging point and establishes a merging sequence by ascending the predicted times-to-go. Besides, the sequence control layer detected possible conflicts by comparing successive values in the ordered set of times-to-go and then assigned appropriate motion control law to a motion control layer. The motion

control layer accordingly generated trajectories for vehicles to reach the predefined merging velocity and have large enough time intervals at the merging point. Moreover, when a merging sequence is predefined or given by mapping vehicles in one lane to another lane, vehicles' are controlled to reach desired inter-vehicle distances at a merging point. Remarkably, V2X communication becomes essential to transmit vehicular information [3]. Different control algorithms, e.g. model predictive control, are proved to plan feasible trajectories for automated vehicles to merge safely with desired speeds or inter-vehicle distance through simulation or field tests [3], [10], [13], [20]. Control strategies for facilitating the merging process with automated vehicles before 2013 are summarized in [21].

2) *Efficient Trajectory Control With Given Sequence or With Simple Sequencing Methods*: Traffic efficiency and operations are then considered in trajectory control strategies for automated vehicles. In [1], a merging sequence was assumed to be given. Merging trajectories were planned for a vehicle by minimizing a cost function, subject to the estimated final states of the vehicle at a merging point. The cost function was a weighted sum of vehicular acceleration, jerk, and its first derivative. The planned trajectories ensured comfort and brought traffic efficiency. In [22], a control zone was presented before a merging zone. CAVs inside the control zone were controlled by a centralized controller. The merging zone was the region with potential lateral collisions of the vehicles. A *first-in-first-out* rule was used to decide merging sequences. If two vehicles entered the control zone simultaneously, the centralized controller randomly selected one to have a smaller vehicle order. Vehicles were assumed to have a constant speed in the merging zone. Only one vehicle could be crossing the merging zone at a time. The controller planned an acceleration trajectory for each vehicle by minimizing a weighted sum of the accelerations during the merging process and the time headway when the vehicles were leaving the merging zone, thus reducing fuel consumption and travel time. In [23], a merging sequence was scheduled by projecting on-ramp vehicles to the right-most mainline lane using a merging point as the reference. A centralized controller planned vehicular trajectories by minimizing a weighted sum of minus speeds and standard deviation of accelerations during the merging process. In [24], a state-constrained optimal control-based trajectory control strategy was proposed. The speeds of mainline facilitating CAVs were bounded from below to mitigate the negative impact on the safety of their following vehicles. However, the aforementioned studies mainly focus on trajectory control and do not explore an optimal or sub-optimal merging sequence.

3) *Efficient Trajectory Control With Vehicle Sequence Optimization*: Without changing trajectory control strategies, an extra improvement in traffic efficiency can be achieved by using an optimal or sub-optimal merging sequence. Generally, different merging sequences can be evaluated when both detailed trajectory control strategies and the actual system behaviour are known. In [25], a merging sequence was given by an assumed command and control center. The merging of two strings of vehicles into a single guideway was reduced to controlling vehicles in a single string. The merging problem

was formulated as an optimal control problem. All possible merging sequences were used to get the corresponding values of the objective function of the optimal control problem. The optimal merging sequence corresponding to the minimum value was chosen. In [26], the upstream vehicle closest to a defined decision point acted as a leader and established merging sequences for its upstream vehicles within the vehicle-to-vehicle (V2V) communication range. Prospective merging sequences were selected based on the estimated arriving times of mainline and on-ramp vehicles to a merging point. With each of the merging sequences, the merging delay was calculated. The one corresponding to the minimum merging delay was selected as optimal. Besides, when checking different merging sequences, interaction-aware maneuver prediction can rely on surrogate linear models. In [27], a tactical layer controller used constrained linear models to predict vehicular trajectories during merging. All possible merging sequences were successively evaluated to find the optimal one. An operational layer controller accepted the given optimal merging sequence and planned vehicular trajectories based on model predictive control. Moreover, sub-optimal merging sequences can be given by using certain assumptions on final vehicular states or rules. In [28], the arrival times of mainline and on-ramp vehicles were assigned to form a merging sequence. The merging sequence was then adjusted according to four rules to have small time intervals between consecutive vehicles. The acceleration profile for each vehicle was generated by minimizing the square of accelerations within the assigned arrival time. If a newly detected vehicle was instructed to follow an existing vehicle in the same lane and had a short inter-vehicle distance with the target, the newly detected vehicle utilized a linear control law to update its acceleration. In [29], a tactical layer controller gave a merging sequence based on two assumptions: 1) CAVs in two platoons traveled with a constant free-flow speed between their initial positions and a merging position. 2) the final platoon settled down to equilibrium at the merging location with all vehicles following Newell equilibrium conditions. A merging sequence was established by projecting initial positions of vehicles with the free-flow speed along a shock wave starting from the merging position. Besides, the tactical layer controller gave time instants when yielding vehicles started to create gaps by increasing time shifts, respectively. An operational layer was designed based on model predictive control (MPC). It received tactical decisions and then planned acceleration trajectories for CAVs. In [30], the first controlled vehicles in a main or an on-ramp lane accelerated to their desired speeds, and following vehicles utilized intelligent driver model (IDM) to update accelerations in a divided game area. When one controlled vehicle was leaving the game area, a centralized controller utilized game theory to give a merging sequence by evaluating the weighted sum of three aspects: 1) the number of vehicles in each lane; 2) a vehicle's distance from a predefined merging point; 3) the mean space distance of a vehicle from its preceding and following one. The weight vector was determined by searching the Pareto solution of minimizing fuel consumption caused by velocity and acceleration, respectively. In a divided adjusting area, vehicles followed their preceding vehicles given in the

merging sequence and utilized constrained IDM to update their accelerations, respectively.

4) *Approaches in Mixed Traffic*: Improving merging efficiency in mixed traffic also draws significant attention. In [17], CAVs in the main lane adjacent to the acceleration lane acted as leaders of different platoons and collected small partial headways to form single longer ones to facilitate merging, thus reducing merging disruption. In [31], a hierarchical model predictive control approach was presented for solving a coordinated and integrated traffic control problem. CAVs were treated as sensors to estimate traffic state and future demands were predicted in an adaptation and prediction layer. The estimation and prediction information were sent to other layers. The optimization layer optimized ramp metering, variable speed limits, and lane-changing control (lateral flows) by solving a convex quadratic programming problem. The local control layer were decentralized feedback controllers which used some values resulting from the optimization layer as set points. These controllers were for ramp metering and variable speed limits. The lane-changing decisions were the same as those computed by the optimization layer. An application layer worked by converting the outcome of the optimization and local control layers. The lane-changing control actions were implemented by sending lane-changing suggestions to an appropriate number of selected vehicles. In [5], the acceleration rates of automated vehicles were determined by using a cooperative intelligent driver model. This model considered the actions of surrounding vehicles. Mainline automated vehicles created larger gaps for on-ramp human-driven vehicles within their detection ranges in advance. As a result, automated vehicles eliminated freeway oscillations. In [32], a ramp merging mechanism was formulated as a bi-level optimization program to give merging sequences and planned vehicular trajectories together. With the mechanism, the throughput can be further increased by 10%-15%. The mechanism could be used for mixed traffic. In [33], two fine lane management approaches for intelligent connected vehicles were proved to reduce delay in highway weaving areas. Both of them entailed guiding vehicles to change lane in advance before entering the weaving sections. One approach added lane-changing separation which utilized a white solid line to constrain lane-changing behaviors of vehicles. And the other approach utilized a conflict avoidance area. In [34], drivers in the connected environment were observed to take more time to complete their lane-changing maneuvers than in the non-connected environment. In [35], a pro-social control strategy for CAVs in multi-lane highway traffic conditions was proposed and a CAV was controlled by considering its and surrounding vehicles' efficiency and comfort. By applying the pro-social control strategy, traffic efficiency and comfort could be improved. In [36], a vehicle lateral stability controller was designed by using MPC. In some studies, lane-changing behaviors of CAVs are described by lane-changing models or rules for human-driven vehicles with or without certain changes [15], [37], [38]. These lane-changing models or rules lack considering possible cooperation among CAVs.

5) *Merging Strategies at on-Ramp Merging Areas With Multiple Main Lanes*: Vehicle sequences in multiple main lanes



can be given by optimizing platoon formation. In [39], a linear model for assigning incoming on-ramp vehicles to appropriate platoons was presented. This linear model maximized the distance that platoons stayed intact and grouped vehicles based on their destinations. On-ramp vehicles entering the highway were only allowed to join the tail end of platoons or initiate a new platoon if no feasible platoon could be found. Mainline vehicles did not change lane to facilitate the lane-changing maneuvers of on-ramp vehicles. Allowing mainline CAVs to change lane to facilitate on-ramp merging increases complexity. In [40], a dynamic adaptive algorithm in a central control unit was introduced to assign vehicle sequences in each main lane. It worked by minimizing a cost function of travel time. The on-ramp vehicle was assumed to accelerate with constant acceleration to reach the speed limits before it merged into mainline traffic at a predetermined merging point. Its possible travel times to arrive at the merging point were calculated by utilizing different constant accelerations. The travel time of a mainline platoon vehicle was calculated by the assumption that it traveled with its current acceleration until reaching its desired speed and then traveled with the desired speed. The desired speed of a platoon follower was the speed of its directly preceding vehicle. For a platoon leader, its desired speed was the speed limits. Based on the estimated travel times of the on-ramp vehicle and the platoon vehicles in the main lane adjacent to the on-ramp lane at the merging point, where the on-ramp vehicle merged into mainline traffic was determined. If a platoon vehicle might have a collision with the on-ramp vehicle based on estimation, it might decelerate with constant deceleration, accelerate, or change lane to the left. It only considered to change lane when a large gap existed in the left main lane and it had large enough inter-vehicle distances for lane changing. All possible alternatives to resolve conflicts based on the estimated travel times were evaluated. If feasible alternatives existed, the one that leads to the minimum travel time was selected as the optimal command at each time step. If none of the alternatives were feasible, the on-ramp vehicle slowed down. The on-ramp vehicle and the chosen feasible alternatives updated their speeds with constant acceleration or deceleration, respectively. Following platoon vehicles updated their accelerations by using a linear equation proposed in [2]. The algorithm was adaptive because it adjusted decisions by using the real-time data of vehicles' status at each time step until an on-ramp vehicle started to turn left. In [41], a rule-based lane-changing decision was utilized for upstream mainline CAVs in the outer main lane in a lane-changing region to balance future downstream lane flow distribution. The rule decided the lane-changing proportion, thus determining the number of mainline vehicles that needed to change lane. Mainline vehicles were then randomly chosen as lane changers. The lane changers' future vehicle sequences were decided by mapping their positions to their target lane. In the lane-changing region, CAVs' trajectories were generated together by maximizing the total speed. In a cooperative merging region, merging sequences were assumed to be given. A CAV's trajectory was planned by maximizing its speed during merging. In [42], a bi-level cooperative driving strategy was utilized to reduce delay. An upper-level planning checked

some promising passing orders generated by Monte Carlo Tree Search. The search was based on some heuristic rules and a passing-order-to-trajectory interpretation algorithm. The passing-order-to-trajectory interpretation algorithm was presented in a lower-level planning. The algorithm gave the total travel time and CAVs' acceleration trajectories. In [43], each vehicle minimized its driving safety, ride comfort, and travel efficiency cost by playing a game. Besides, an on-ramp CAV and its two adjacent passive participants in two different main lanes: a follower in its adjacent main lane and the follower of the mainline vehicle in the left main lane, played in a cooperative game to check whether extra total cost could be reduced without sacrificing each vehicle's benefit. The vehicle in the right main lane may change lane to the left to further reduce the total cost. Driving characteristics of the CAVs could be considered. Different driving characteristics brought different optimal choices for CAVs. In [44], estimated delay time in an induction zone of mainline was minimized by instructing some upstream controlled CAVs in the rightmost main lane to change lane to the left. On-ramp CAVs joined outer mainline traffic in the merging zone by using a *first-in-first-out* principle. The earliest and latest time instants for on-ramp CAVs to join mainline traffic at a fixed position were calculated based on vehicular initial position, speed, and allowed acceleration range, respectively. Their joining time instants were optimized together to make on-ramp vehicles join mainline traffic quickly and reduce affected CAVs' delay.

### B. Knowledge Gap

In summary, trajectory control methods, merging or vehicle sequences selections, and mainline facilitating lane-changing maneuvers affect traffic efficiency or traffic operations during merging. By comparison, the first two aspects are extensively studied. When CAVs travel in multiple main lanes near on-ramps, allowing mainline vehicles to change lane for facilitating merging increases both flexibility to create large spaces for merging vehicles and complexity of the controlled system. Existing control methods only allow upstream mainline vehicles to change lane to the left before entering a given merging zone or without cooperation, check several possible vehicle sequence combinations based on safe lane-changing constraints and with an assumption that each CAV has constant acceleration in the process, or allow at most three CAVs to play a game without sacrificing each CAV's benefit. These methods restrict lane change locations, ignore chances for CAVs to cooperatively create safe lane-changing conditions, or fail to optimize overall traffic efficiency. A centralized control method is needed to systematically address lane-changing maneuvers of mainline CAVs to optimize overall traffic performance during on-ramp merging.

### C. Our Contribution

This paper proposes a hierarchical cooperative merging control approach to address automated merging procedures of on-ramp vehicles when mainline CAVs are allowed to change lane to facilitate the on-ramp merging process. Main contributions are summarized as follows: (i) The maneuver planner centrally

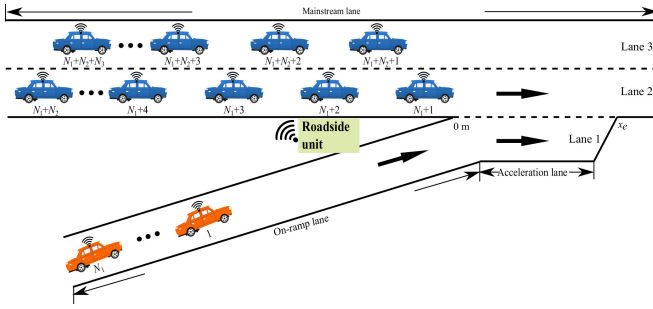


Fig. 1. Schematic illustration of a typical on-ramp merging scenario with multiple main lanes.

predicts future merging procedures in a long time horizon  $T$ , e.g.  $T \geq 50$  s, by using a uniform prediction model to represent *car-following*, *cruising*, and *cooperative lane-changing* maneuvers during merging and optimizes dynamic vehicle sequences in each lane by minimizing disturbances reflected by negative acceleration to upstream traffic [45]. The prediction model is constructed based on linear microscopic traffic models. Mainline CAVs' lane-changing positions are not restricted and potential vehicle sequences are not restricted by initial vehicular states. (ii) The operational trajectory controller centrally regulates vehicle accelerations by using MPC in a short time horizon  $T_p$ , e.g.  $T_p = 6$  s, and decides the time instants for lane changers to turn left. The predictive and feedback nature of the MPC scheme can check the feasibility of established vehicle sequences and handle predicted possible failures in time. (iii) Both the planner and operational controller consider vehicle-vehicle interaction and constraints on acceleration and speed to have safe and feasible dynamics.

#### D. Paper Organization

The remainder of the paper is organized as follows. Section 2 presents the hierarchical cooperative merging control approach. Section 3 and Section 4 elaborate on the mathematical formulations of the planner and operational controller, respectively. Section 5 presents the simulation setup and experimental results. Finally, Section 6 concludes the contribution.

## II. HIERARCHICAL COOPERATIVE MERGING CONTROL APPROACH

A typical on-ramp merging scenario (See Fig. 1) has two main lanes, one on-ramp lane, and one acceleration lane. The lanes are numbered from right to left, with the on-ramp lane and the acceleration lane both numbered 1. On-ramp CAVs have to merge into mainline traffic, thus having path conflicts with mainline CAVs in lane 2.

The hierarchical cooperative merging control approach (See Fig. 2) resolves possible conflicts by regulating both mainline and on-ramp CAVs' trajectories to have large enough inter-vehicle distances during merging near on-ramps. Both the planner and operational controller are in a roadside unit (See Fig. 1 and Fig. 2), so that the trajectories of all CAVs can be controlled together. The roadside unit collects initial vehicle sequence, position, and speed through vehicle-to-infrastructure

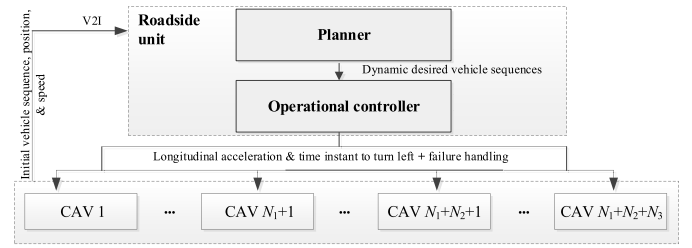


Fig. 2. Cooperative control hierarchy for maneuver planning and trajectory control of CAVs near on-ramps.

(V2I) communications, and decides to control which CAVs. Initially, the last two CAVs in lane 2 and lane 3 controlled by the roadside unit can be followed by upstream vehicles, the last vehicles of platoons, or the last upstream CAVs detected by the roadside unit. If many CAVs in lane 2 are behind the last upstream on-ramp CAV longitudinally, the last CAV in lane 2 is the second upstream CAV that is longitudinally behind the last upstream on-ramp CAV. The last CAV in lane 3 is a possible future follower of all possible lane changers in lane 2 if many upstream CAVs in lane 3 are close to the last vehicle in lane 2. The possible following vehicles upstream of the last CAVs under control in the two main lanes are assumed to be able to ensure string stability. A platoon has string stability if the variation of speed reduces over the vehicle number in the platoon [46].

The planner utilizes model-based prediction and decides dynamic vehicle sequences in each lane by considering the mandatory lane-changing demand of on-ramp vehicles and by minimizing overall disturbances to upstream mainline traffic during prediction time horizon  $T$ . The dynamic vehicle sequences are then sent to the operational controller which commands longitudinal acceleration for CAVs and time instants to turn left for lane changers, respectively. On-ramp CAVs merge into mainline traffic before reaching the end of the acceleration lane.

The  $T$  in the planner is up to 50 seconds (s). The planner updates its decision at low frequencies, e.g. every 5-10 s. The operational controller updates the command at high frequencies, e.g. every  $dt \leq 0.1$  s. To explore optimal vehicle trajectories near on-ramps, centralized control methods are utilized by the planner and operational controller. However, the hierarchical cooperative merging control approach is not restricted to centralized control methods and it can be extended to adapt to mixed traffic. If the operational controller finds that an on-ramp CAV does not have large enough inter-vehicle distances with its target preceding and following CAVs for lane changing when it is approaching the end of the acceleration lane based on prediction, the operational controller overrules the given vehicle sequence for the on-ramp vehicle to find feasible and safe trajectories.

## III. MANEUVER PLANNER: MODEL-BASED OPTIMIZATION STRATEGY

The merging of on-ramp CAVs in lane 1 into mainline traffic is mandatory. The planner thus has to give feasible dynamic vehicle sequences where the on-ramp CAVs can merge into

mainline traffic before reaching the end of the acceleration lane. The planner answers under which conditions mainline CAVs change lane to facilitate merging attenuates disturbances to upstream traffic, which mainline vehicles change lane, and what the final vehicle orders of the mainline lane changers are. Time argument  $t$  is omitted to improve readability when no ambiguity exists.

All CAVs that are controlled by the planner and the operational trajectory controller are numbered from 1 to  $N_1 + N_2 + N_3$  (See Fig. 1).  $N_i$  represents the initial number of CAVs in lane  $i$ .  $O_{i,j}$  and  $P_{i,j}$  are 0-1 variables.  $O_{i,j}$  denotes the vehicle sequence between CAV  $i$  and  $j$  based on all CAVs' lateral and longitudinal positions.  $O_{i,j} = 1$  indicates that CAV  $i$  is CAV  $j$ 's directly preceding vehicle in the same lane. Otherwise,  $O_{i,j} = 0$ .  $P_{i,j}$  denotes the desired vehicle sequence between CAV  $i$  and  $j$  according to the planner.  $P_{i,j} = 1$  indicates that CAV  $i$  is CAV  $j$ 's target directly preceding vehicle. All CAVs in lane 1 have to change lane safely before reaching the end of the acceleration lane. To this end, at  $T$ ,  $\sum_{i=1}^{N_1} \sum_{j=1}^{N_1+N_2+N_3} O_{i,j} + \sum_{i=1}^{N_1+N_2+N_3} \sum_{j=1}^{N_1} O_{i,j} \geq N_1$ .

#### A. Linear Bounded Models for Merging Prediction

The longitudinal behavior of a CAV is expressed by a second-order vehicle dynamics model. The open-loop system dynamics for each vehicle are described in (1), where  $x_i$ ,  $v_i$ , and  $a_i$  denote the location, speed, and acceleration of CAV  $i$ , respectively.

$$\dot{x}_i = v_i, \dot{v}_i = a_i, \quad i = 1, 2, \dots, N_1 + N_2 + N_3 \quad (1)$$

To predict vehicular trajectories during the future merging process, the planner borrows models from the traffic flow community to represent CAVs' behavior during the on-ramp merging process. Considering cases when vehicle may conflict with or directly influence each other, vehicles' motions are categorized into three maneuvers: *car-following*, *cruising*, and *cooperative lane-changing*.

The *car-following* maneuver works when a vehicle follows its future directly preceding vehicle which is in the same lane, i.e.,  $O_{j,i} = P_{j,i}$ . The *car-following* operation is modeled using a car-following model used in [2] for automated vehicles with bounded accelerations, as shown in the car-following part in the prediction model shown in (2). The *cruising* maneuver applies to the first vehicle in each lane according to the dynamic vehicle sequences and its formulation is as shown in the cruising part in (2), where  $v_i^{\text{limits}}$  can also be replaced with the desired speed set by a driver or traffic control system. The *cooperative lane-changing* maneuver computes the accelerations in the cooperative lane-changing process as a special case of car-following maneuver. When a vehicle's target lane is the left of its original lane according to the dynamic vehicle sequences, it starts to prepare itself to create sufficient inter-vehicle distances to execute lane change. To achieve large enough inter-vehicle distances, it and its future directly follower in the target lane are in the cooperation maneuver until it accomplishes the lane change. The cooperation maneuver is

formulated in the cooperative lane-changing part in (2).

$$\begin{aligned} a_i = & \underbrace{P_i^B \cdot [(D_1 \cdot \Delta V_i + D_2 \cdot \Delta S_i + D_3 \cdot a_j)]}_{\text{car following}} \\ & + \underbrace{P_i^C \cdot [(D_5 \cdot \Delta V_i + D_6 \cdot \Delta S_i + D_7 \cdot a_j)] \cdot (1 - P_i^B)}_{\text{cooperative lane-changing}} \\ & + \underbrace{(1 - P_i^C) \cdot D_4 \cdot \Delta V_i}_{\text{cruising}} \end{aligned} \quad (2)$$

where,  $D_1, D_2, D_3, D_4, D_5, D_6$ , and  $D_7$  are model parameters;  $P_i^C = \sum_{j=1}^{N_1+N_2+N_3} P_{j,i}$  and  $P_i^B = \sum_{j=1}^{N_1+N_2+N_3} (P_{j,i} \cdot O_{j,i})$ ;  $\Delta V_i = (1 - \sum_{j=1}^{N_1+N_2+N_3} P_{j,i}) \cdot v_i^d + \sum_{j=1}^{N_1+N_2+N_3} (v_j \cdot P_{j,i}) - v_i$  and  $\Delta S_i = s_i - s_i^d$  are the relative speed and gap error of vehicle  $i$  with respect to its future directly preceding vehicle based on the scheduled vehicle sequences in each lane, respectively;  $s_i = (1 - \sum_{j=1}^{N_1+N_2+N_3} P_{j,i}) \cdot (s_i^d + x_i + l_{veh}) + \sum_{j=1}^{N_1+N_2+N_3} (x_j \cdot P_{j,i}) - x_i - l_{veh}$ ;  $l_{veh}$  denotes vehicle length,  $s_i^d = v_i \cdot t^d + s_0$  is the desired gap of CAV  $i$ , and  $v_i^d$  is the desired speed if no predecessor exists.  $t^d$  and  $s_0$  represent the desired time gap and the minimum inter-vehicle gap at standstill, respectively.  $P_i^C$  and  $P_i^B$  are equal 0 or 1. If vehicle  $i$  has a desired preceding vehicle,  $P_i^C$  is 1. When vehicle  $i$  is in the cruising maneuver, it does not have a desired preceding vehicle and  $P_i^C = 0$ .  $P_i^B$  is 1 when vehicle  $i$  follows its desired preceding vehicle in its target lane. In (2), the value of  $P_i^B + P_i^C \cdot (1 - P_i^B) + (1 - P_i^C)$  is 1. If  $P_i^B$  is 1, CAV  $i$  is in the car-following maneuver. If  $P_i^C = 0$  or  $(1 - P_i^C) = 1$ , CAV  $i$  is in the cruising maneuver and it travels to achieve or keep its desired speed. If  $P_i^C \cdot (1 - P_i^B) = 1$ , that is  $P_i^C = 1$  and  $P_i^B = 0$ , CAV  $i$  travels in a different lane from that of its desired directly preceding vehicle and it is in the cooperative-lane-changing maneuver.

The acceleration calculated by the *car-following* and *cooperative lane-changing* maneuvers are bounded to  $[a_{\min}, a_i^s]$  to be reasonable and safe, where  $a_{\min}$  is the minimal negative acceleration, and  $a_i^s$  is the lower bound of maximum acceleration  $a_{\max}$  and vehicle-vehicle interaction acceleration  $a_i^{\text{int}}$  shown in (3).

$$\begin{aligned} a_i^{\text{int}} = & \sum_{j=1}^{N_1+N_2+N_3} ((D_1 \cdot \Delta V_i^o + D_2 \cdot \Delta S_i^o \\ & + D_3 \cdot a_j) \cdot (1 - (\Delta S_i^o \leq 0 \wedge a_j < 0)) \cdot O_{j,i}) \end{aligned} \quad (3)$$

where,  $\Delta V_i^o = (1 - \sum_{j=1}^{N_1+N_2+N_3} O_{j,i}) \cdot v_i^d + \sum_{j=1}^{N_1+N_2+N_3} (v_j \cdot O_{j,i}) - v_i$  and  $\Delta S_i^o = (1 - \sum_{j=1}^{N_1+N_2+N_3} O_{j,i}) \cdot (v_i \cdot t_{\min}^d + s_0 + x_i + l_{veh}) + \sum_{j=1}^{N_1+N_2+N_3} (x_j \cdot O_{j,i}) - x_i - l_{veh}$  are the relative speed and gap error of vehicle  $i$  with respect to its current directly preceding vehicle, respectively; and,  $t_{\min}^d$  is the minimum safe time gap. When a vehicle is decelerating, its directly following vehicle in its original lane does not accelerate if their inter-vehicle distance is less than the follower's desired value.

#### B. Acceptable Time Gaps for Changing Lane

When inter-vehicle distances between a lane-changer and both its future directly preceding and following vehicle are large enough, it changes lane. For on-ramp lane changers



traveling in the acceleration lane, they accept a smaller but safe time gap to change lane while approaching the end of the acceleration lane, which is reflected by an acceptable time gap  $t^{atg}$  shown in (4) [27].  $x_e$  (See Fig. 1) stands for the end of the acceleration lane. For a mainline lane changer, it accepts  $t_{\min}^d$  to accomplish its merging maneuver. When lane-changing conditions are met, lane-changers start to steer to the left, with a fixed time duration  $t_m$  [27], [47]; after  $0.5 \cdot t_m$ , the lane-changer is in its target lane.

$$t^{atg} = x_i \cdot (t_{\min}^d - t^d) / x_e + t^d; \quad (4)$$

### C. Optimization Problem Formulation: Dynamic Vehicle Sequences

The planner is a model-based optimization model that optimizes dynamic vehicle sequences by minimizing disturbances to upstream traffic and by explicitly ensuring successful lane-changing of on-ramp vehicles. Its state vector is represented by  $\mathbf{Z}^P = (x_1, y_1, v_1, a_1, \dots, x_{N_1+N_2+N_3}, y_{N_1+N_2+N_3}, v_{N_1+N_2+N_3}, a_{N_1+N_2+N_3})^T$  and the control vector  $\mathbf{U}^P = (P_{1,1}, \dots, P_{N_1+N_2+N_3, N_1+N_2+N_3})^T$  shows time-varying vehicle sequence for every two vehicles in each lane, where  $y_i$  denotes lateral position of CAV  $i$ .

Vector  $Q_2$  and  $Q_3$  representing negative accelerations of the last vehicles in main lane 2 and 3 respectively in  $T$  are chosen to reflect disturbances to upstream traffic and the Euclidean norm (or 2-norm) of them is included in the performance measure shown in (5) [45]. Given that On-ramp CAVs are mandatory to change lane, a vector  $M = [m_1, \dots, m_{N_1}]^T$  and a binary vector  $B = [b_1, \dots, b_{N_1}]^T$  are introduced, where  $m_i$  is a large number and  $b_i = 0$  means that on-ramp vehicle  $i$  has accomplished merging within  $T$ . To this end,  $b_i = (\sum_{j=1}^{N_1+N_2+N_3} (O_{i,j} \cdot P_{i,j}) + \sum_{j=1}^{N_1+N_2+N_3} (O_{j,i} \cdot P_{j,i}) \equiv 0)$  at  $T$ .

$$\min_{U^P} (\|Q_2\|_2 + \|Q_3\|_2 + M^T \cdot B) \quad (5)$$

subject to:

- the system dynamics model shown in (1), maneuver prediction model shown in (2).
- the initial condition:  $\mathbf{Z}^P(0) = \tilde{\mathbf{Z}}^P(0)$  and  $\sum_{i=1}^{N_1+N_2+N_3} \sum_{j=1}^{N_1+N_2+N_3} P_{i,j}(0) = N_1 + N_2 + N_3 - 3$ .
- the final condition:  $N_1 + N_2 + N_3 - 2 \leq \sum_{i=1}^{N_1+N_2+N_3} \sum_{j=1}^{N_1+N_2+N_3} P_{i,j}(T) \leq N_1 + N_2 + N_3 - 1$ .
- speed constraints:  $0 \leq v_i \leq v_{\text{limits}}$ .
- acceleration constraints:  $a_{\min} \leq a_i \leq a_i^s$ .

where,  $\tilde{\mathbf{Z}}^P(0)$  is initial state at 0 s.

(5) is a generic formulation. Extra assumptions can be made to reduce randomness and freedom of lane-changing choices of mainline CAVs. To restrict lane-changing times of CAV  $i$  during  $T$ , the sum of the absolute values of lateral position changes can be constrained. Besides, lane-changing directions can be restricted to reduce complexity. In section V, only a limited number of CAVs are considered with different initial settings, and thus (5) can be solved effectively using enumeration. However, more efficient solution methods are left to be explored for situations where enumeration is difficult or time-consuming.

### IV. OPERATIONAL TRAJECTORY CONTROLLER: MODEL PREDICTIVE CONTROL APPROACH

The operational controller optimizes vehicle trajectories by taking into account the dynamic vehicle sequences established by the planner. It is formulated as model predictive control to regulate longitudinal acceleration trajectory to reach desired vehicular states and to safely lead lane changers to their target lanes, respectively.

The desired vehicular state for the first vehicle in each lane is to reach the desired speed. The following vehicles wish to have the same speed as their directly predecessor in target lane while keeping safe or the desired inter-vehicle distances, respectively. To this end,  $\mathbf{Z}^o = (\Delta V_1, s_1, \Delta y_1, \dots, \Delta V_{N_1+N_2+N_3}, s_{N_1+N_2+N_3}, y_{N_1+N_2+N_3})^T$  is defined as the state vector.  $\Delta y_i = y_i^t - y_i$  is deviation between the target and actual lateral position of vehicle  $i$ . If  $\Delta y_i$  is not 0, vehicle  $i$  changes lane when  $\xi_i = 1$  and the lane-changing direction depends on  $\Delta y_i$ .  $\xi_i$  stands for the safe lane-changing acceptability for vehicle  $i$  and is evaluated by the operational controller based on the planned acceleration trajectories and predicted vehicular positions. The control vector is defined as  $\mathbf{U}^o = (a_1, \xi_1, \dots, a_{N_1+N_2+N_3}, \xi_{N_1+N_2+N_3})^T$ .

An optimal  $\mathbf{U}^o$  in a finite time horizon  $[t_0, t_0 + T_p]$  is given by minimizing a constructed objective function as shown in (6). The constructed objective function penalizes deviations of vehicular states to equilibrium states where the first vehicles in each lane travel to reach desired speeds and following vehicles travel at desired inter-vehicle distances, with the same speed with directly preceding vehicles, and with zero accelerations, as shown in (7). The minimization of the three types of deviations leads vehicles to longitudinally reach their equilibrium states gradually. Lateral decisions are established based on the planned longitudinal acceleration trajectory.  $\xi_i$  is 1 when the predicted inter-vehicle distances are larger than the accepted inter-vehicle distances of vehicle  $i$  for changing lane during  $T_p$ . The inter-vehicle distances between vehicle  $i$  with both its direct predecessor and follower in the target lane are considered. The accepted inter-vehicle distance for lane changing is the same as given in III-B. When  $\Delta y_i$  is not 0 and  $\xi_i$  is 1, vehicle  $i$  starts to turn to its target lane. A lane changer follows a polynomial equation with a fixed time duration  $t_m$  to accomplish merging [27], [47].

$$\begin{aligned} \min_{\mathbf{U}^o} \zeta(\mathbf{Z}^o, \mathbf{U}^o) &= \min_{\mathbf{U}^o} \left( \int_{t_0}^{t_0+T_p} \psi(\mathbf{Z}^o, \mathbf{U}^o) dt \right) \quad (6) \\ \psi &= c_1 \cdot \sum_i (s_i - s_i^d)^2 + c_2 \cdot \sum_i \Delta v_i^2 + c_3 \\ &\quad \cdot \sum_i a_i^2 \\ &= c_1 \cdot (X_1 - S^d)^2 + c_2 \cdot X_2^2 + c_3 \cdot A^2 \quad (7) \end{aligned}$$

subject to:

- the system longitudinal dynamics model shown in (1).
- an initial state:  $\mathbf{Z}^o(t_0) = \tilde{\mathbf{Z}}^o(t_0)$ .
- speed constraints:  $0 \leq v_i \leq v_{\text{limits}}$ .
- gap constraints:  $s_i \geq s_0 \cdot \sum_{j=1}^{N_1+N_2+N_3} P_{j,i}$ .
- acceleration constraints:  $a_{\min} \leq a_i \leq a_i^{sp}$ .  $a_i^{sp}$  is the maximum value of  $a_{\max}$  and the first value of the optimal

solution to the following optimization problem:

$$\min_{\mathbf{a}_i^*} \int_{t_0}^{t_0+T_p} \sum_{j=1}^{N_1+N_2+N_3} ((c_1 \cdot \Delta V_i^{o2} + c_2 \cdot \Delta S_i^{o2} + c_3 \cdot a_i^2) \cdot (1 - (\Delta S_i^o \leq 0 \wedge a_j < 0)) \cdot O_{j,i}) dt$$

where,  $\tilde{\mathbf{Z}}^0(t_0)$  is the value of the state vector at updated time instant  $t_0$ . The initial value of  $t_0$  is 0 s. Given  $\Delta t$  as the control time step of the operational controller, the control command is updated every  $\Delta t$  and  $t_0$  are multiples of  $\Delta t$ . With  $\mathbf{X}_1 = (s_1, \dots, s_{N_1+N_2+N_3})^T$ ,  $\mathbf{S}^d = (s_1^d, \dots, s_{N_1+N_2+N_3}^d)^T$ ,  $\mathbf{X}_2 = (\Delta v_1, \dots, \Delta v_{N_1+N_2+N_3})^T$ , and  $\mathbf{A} = (a_1, \dots, a_{N_1+N_2+N_3})^T$ , vehicle longitudinal dynamics can be described by (8).

$$\begin{pmatrix} \mathbf{P}^1 \cdot \dot{\mathbf{X}}_1 \\ \dot{\mathbf{X}}_2 \end{pmatrix} = \begin{pmatrix} \mathbf{P}^1 \cdot \mathbf{X}_2 \\ (\mathbf{P}^2)^T \cdot \mathbf{A} - \mathbf{A} \end{pmatrix} \quad (8)$$

where,

$$\mathbf{P}^1 = \begin{bmatrix} P_1^C & 0 & 0 \\ 0 & \ddots & 0 \\ 0 & 0 & P_{N_1+N_2+N_3}^C \end{bmatrix},$$

$$\mathbf{P}^2 = \begin{bmatrix} P_{1,1} & \cdots & P_{1,N_1+N_2+N_3} \\ \vdots & \ddots & \vdots \\ P_{N_1+N_2+N_3,1} & \cdots & P_{N_1+N_2+N_3,N_1+N_2+N_3} \end{bmatrix}$$

#### A. Solution to the Optimal Control Problem

(6) is solved by using Pontryagin's Minimum Principle [10], [29], [48]. The corresponding Hamiltonian function of the optimization problem is created as shown in (9).

$$\mathcal{H} = c_1 \cdot (\mathbf{X}_1 - \mathbf{S}^d)^2 + c_2 \cdot \mathbf{X}_2^2 + c_3 \cdot \mathbf{A}^2 + \lambda_1^T \cdot \mathbf{P}^1 \cdot \mathbf{X}_2 + \lambda_2^T \cdot ((\mathbf{P}^2)^T \cdot \mathbf{A} - \mathbf{A}) \quad (9)$$

where,  $\lambda_1$  and  $\lambda_2$  are co-state cost of the first-order differential equations of  $\mathbf{P}^1 \cdot \mathbf{X}_1$  and  $\mathbf{X}_2$ , respectively. The necessary conditions for the optimal solutions are listed in (10), with initial state  $\mathbf{Z}^0(t_0)$  given, final time  $t_0 + T_p$  specified, and  $\lambda_1(t_0) = 0$ ,  $\lambda_2(t_0) = 0$ ,  $\lambda_1(t_0 + T_p) = 0$ , and  $\lambda_2(t_0 + T_p) = 0$ . We are then faced with a two-point boundary-value problem which is solved by using an iterative algorithm presented in detail in [29].

$$\begin{aligned} a_i^* &= \arg \min_{a_i} \mathcal{H} \\ -d\lambda_1/dt &= \partial \mathcal{H} / \partial (\mathbf{P}^1 \cdot \mathbf{X}_1) \\ -d\lambda_2/dt &= \partial \mathcal{H} / \partial \mathbf{X}_2 \end{aligned} \quad (10)$$

## V. EXPERIMENT AND NUMERICAL RESULTS

A micro-simulation environment is built by coding in MATLAB R2018a. The proposed hierarchical cooperative merging control approach is then tested and validated under different merging scenarios in the simulation environment.

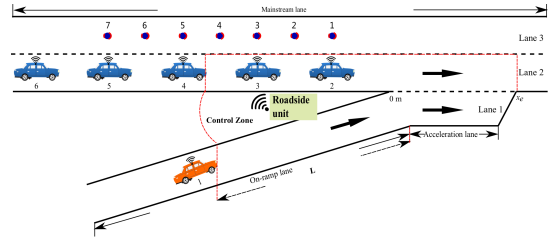


Fig. 3. Choices of initial position for the leader of inner platoon.

#### A. Simulation Setup

Fig. 1 and Fig. 3 present the basic configuration of the simulated highway on-ramp segment. Initially four CAVs are in lane 3 ( $N_3 = 4$ ), five CAVs are in lane 2 ( $N_2 = 5$ ), and one CAV is considered in the on-ramp lane ( $N_1 = 1$ ).

To clearly understand when a CAV changes lane brings extra improvement in traffic operations, the following assumptions are made: 1) only one CAV in lane 2 may be instructed to change lane to lane 3 for facilitating the merging process; 2) CAVs in lane 3 are not allowed to change lane to the right in the merging section; 3) the on-ramp CAV has a following CAV after merging, i.e.  $\sum_{j=1}^{N_1+N_2+N_3} P_{1,j} = 1$ . These assumptions reduce feasible dynamic vehicle sequences to (5), and thus it can be solved effectively using enumeration.

To validate whether extra improvement in traffic operations can be brought, the proposed hierarchical cooperative merging control approach is compared with a control method that uses a *first-in-first-out* rule to establish merging sequences and the operational controller to regulate acceleration. The control zone used by the *first-in-first-out* rule is plotted with red dotted lines in Fig. 3. A vehicle entering into the control zone first is instructed to leave first. When two vehicles enter into the control zone together, priority is given to the mainline vehicle. Vehicles in lane 2 are not instructed to change lane to lane 3. To avoid confusion, the selected control method for comparison is called the *first-in-first-out* method. Besides, a lower-level steering and longitudinal control controller is assumed to follow the planned trajectories precisely without any delay. IDM (See (11)) is used to describe the longitudinal dynamics of the following vehicles upstream of vehicle 6 and vehicle 10 [49]. In (11),  $v$  is speed,  $\alpha$  is the maximum acceleration;  $b$  is the desired deceleration;  $v_p$  is speed of the vehicle's directly preceding vehicle;  $T^f$  is time gap;  $s^*(v, v - v_p)$  is the desired minimum gap, and  $s$  is the actual gap.

$$\begin{aligned} \frac{dv}{dt} &= \alpha \cdot [1 - (\frac{v}{v_{\text{limits}}})^4 - (\frac{s^*(v, v - v_p)}{s})^2] \\ s^*(v, v - v_p) &= s_0 + v \cdot T^f + \frac{v \cdot (v - v_p)}{2 \cdot \sqrt{\alpha \cdot b}} \end{aligned} \quad (11)$$

The initial setting for CAVs includes vehicular position, speed, and desired time gap at 0 s. 528 different initial settings are chosen. The on-ramp CAV initially starts from the upstream boundary of the control zone  $-L$  (See Fig. 3). Two distinguishable situations are considered based on the initial longitudinal position of the on-ramp CAV 1, mainline CAV 4 and 5: (a) the on-ramp CAV has the same value as mainline CAV 4

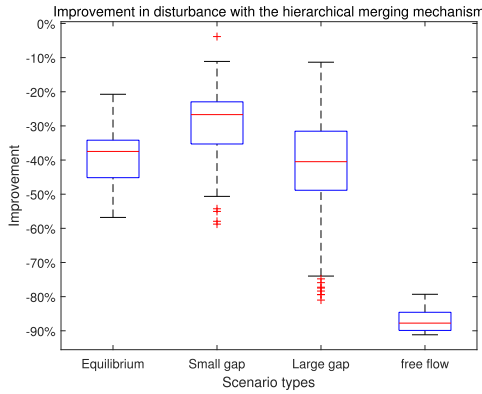


Fig. 4. Performance comparison between the proposed hierarchical cooperative merging control approach and the *first-in-first-out* method.

(See Fig. 3), and (b) the on-ramp CAV is in the middle of the two mainline CAVs (See Fig. 1). The initial speed of the on-ramp CAV entering into the control zone is given 15 m/s, 20 m/s, or 25 m/s.

The desired time gap for all CAVs is set to be 0.6 s, 0.8 s, 1 s, or 1.2 s. CAVs' initial speeds in lane 2 are 25 m/s and inter-vehicle distances are desired values. CAV 2 keeps 25 m/s. Given inter-vehicle distances, CAV 1's position, and (a) or (b), the initial vehicular positions of CAVs in lane 2 are set by calculation.

Two types of situations are constructed in lane 3: (i) free flow where CAVs travel with speed limits respectively and are sparsely distributed; and (ii) crowded traffic where CAVs are traveling with speeds lower than the speed limits and are affected by their directly preceding vehicles in the same lane. For the free flow situation, the CAVs in lane 3 travel with  $v_{\text{limits}}$ , 30 m/s, and are far away downstream. By comparison, for the crowded traffic situation, CAVs in lane 3 travel with 25 m/s and are close to CAVs in lane 2. The longitudinal position of the first CAV in lane 3, CAV 7, is given 7 potential positions which are shown with numbered dots in Fig. 3. Starting from a dot with an odd number, it longitudinally has the same position as a mainline CAV in lane 2; otherwise, it is in the middle of two consecutive mainline CAVs. The initial inter-vehicle distance for CAV 8 is given three different options: equilibrium state, a large gap, or a small gap, with the time gap being 1, 2, or 0.5 times of its desired value, respectively.

The parameters selected for the defined variables are based on published literature or off-line calibration [27], [49].  $T = 50$  s,  $\Delta t = 0.5$  s,  $T_p = 6$  s,  $\Delta t = 0.1$  s,  $L = 62$  m,  $v_{\text{limits}} = 30$  m/s,  $s_0 = 2$  m,  $l_{\text{veh}} = 4$  m,  $t_m = 2$  s,  $D_1 = 0.2$ ,  $D_2 = 0.7$ ,  $D_3 = 0.6$ ,  $D_4 = 0.8$ ,  $D_5 = 0.2$ ,  $D_6 = 0.5$ ,  $D_7 = 0$ ,  $a_{\text{max}} = 2$  m/s<sup>2</sup>,  $a_{\text{min}} = -4$  m/s<sup>2</sup>,  $x_e = 300$  m,  $t_{\text{min}}^d = 0.25$  s,  $c_1 = 0.1$ ,  $c_2 = 0.5$ ,  $c_3 = 0.5$ ,  $\alpha = 1.5$  m/s<sup>2</sup>,  $b = 2$  m/s<sup>2</sup>, and  $T^f = 1.2$  s. The simulation time is 50 s.

### B. Overall Simulation Results

Fig. 4 presents the overall performance comparison between the proposed hierarchical cooperative merging control approach and the *first-in-first-out* method, by considering the

generated disturbances to upstream traffic caused by utilizing the two control methods throughout the simulation, respectively. The reduction rate is calculated by dividing the difference between them by the disturbances caused by using the *first-in-first-out* method and then multiplying the answer by 100. The negative values, from -11% to -91%, show the reduction in disturbances with the hierarchical cooperative merging control approach.

The *first-in-first-out* method assigns the on-ramp CAV to follow CAV 4 under all simulation scenarios. By comparison, the hierarchical cooperative merging control approach schedules different dynamic vehicle sequences based on all CAVs' vehicular states. Under equilibrium scenarios, it tends to make CAV 1 accelerate to a higher speed if CAV 1's initial speed is low or gives CAV 1 a small vehicle order in lane 2, without making a mainline CAV change lane. For the remaining simulation scenarios, when no mainline CAV is instructed to change lane, vehicular states in lane 3 do not influence the scheduled merging sequences and thus the merging sequences are given the same as the equilibrium scenarios, respectively. Under small gap scenarios, for 70 out of the 168 scenarios, a mainline CAV in lane 2 is instructed to change lane to lane 3. For the 70 scenarios, mainline lane changers' final vehicle sequence in lane 3 is 3 under 14 scenarios and 2 under 54 scenarios. Because the existence of small gaps introduces extra disturbances to lane 3 compared with the equilibrium scenarios, the average reduction in disturbances does not excel the equilibrium scenarios obviously (See Fig. 4). However, instructing a mainline CAV in lane 2 to change lane when a small gap exists in lane 3 during merging may bring extra benefits, which is shown by the outliers in Fig. 4. Obviously, a large reduction rate in disturbances shows up when a large space exists in lane 3. The average reduction rates in disturbances for the large gap are bigger than equilibrium scenarios, even though large gaps, like the small gaps, also introduce extra disturbances to lane 3. Under the large gap scenarios, a mainline CAV in lane 2 is instructed to change lane during merging for 109 out of the 168 scenarios. For the 109 scenarios, mainline lane changers' final vehicle sequence in lane 3 is 3 under 6 scenarios and 2 under 103 scenarios. Compared with the small gap scenarios, large gap scenarios have a higher potential to further reduce disturbances through lane-changing behavior of mainline CAVs (See Fig. 4). Based on the final vehicle sequences of the lane changers in lane 3 under the small gap and large gap scenarios, the lane changers are instructed to target the existing small or large gaps in lane 3 for lane changing with high possibilities. For the free flow scenarios, the on-ramp CAV occupies the gap created by a lane changer in lane 2, thus bringing even bigger reduction rates in disturbances.

Fig. 5 visualizes the correlation between lane-changing time instants of the on-ramp CAV and the mainline lane changers under the 109 large gap scenarios and free flow scenarios. Under these scenarios, CAV 1's lane change time is at least 1 s later than the mainline lane changer. Noticeably, mainline lane changers are given 2 s to accomplish lane changing. 1 s after their lane change time instants, they have already left lane 2, respectively. To this end, the on-ramp CAV 1 starts to change

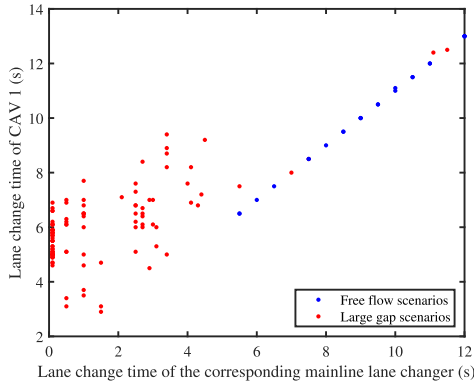


Fig. 5. Correlation between lane change time of CAV 1 and the corresponding mainline lane changer under the 109 large gap scenarios and free flow scenarios.

lane after mainline lane changers have left lane 2, respectively. This indicates that disturbances to upstream traffic in lane 2 can reduce with a large gap following or being utilized by CAV 1. Under free flow scenarios, the deviation of the mainline and on-ramp lane changers' lane-changing time instants is 1 s and CAV 1 utilizes the slots created by mainline lane changers for merging. For free flow scenarios, lane changers do not bring extra disturbances to lane 3; thus, the control target relaxes to reduce disturbances to upstream traffic in lane 2. A small vehicle order is given to CAV 1 to further reduce disturbances. The mainline lane changers start to change lane when CAV 1's target lane changes to lane 2. The differences in lane-changing time instants for mainline lane changers are caused by the differences in on-ramp CAV 1's initial speed and position. For the 109 large gap scenarios, the behavior of a mainline lane changer may reduce disturbances in lane 3. As a result, the lane-changing time instants for lane changers are results of trade-offs to have minimal disturbances to upstream traffic.

### C. A Large Gap Scenario

The performance of the hierarchical cooperative merging control approach is presented in detail for a large gap scenario. The large gap scenario has the following initial settings: 1) all CAVs start from 25 m/s; 2) the on-ramp CAV's position type is (b); 3) longitudinal position of 7 starts from dot 2 in Fig. 3; 4) the desired time gap is 1 s; 5) vehicle 6 and vehicle 10 are followed by vehicle f2 and vehicle f3, respectively; and 6) vehicle f2 and vehicle f3 start from 25 m/s and their initial inter-vehicle distances are 36 m.

1) *Planner Results*: Before 0.5 s, the planner instructs no CAV to change its target lane. At 0.5 s, the CAV 3 is instructed to follow CAV 7. At 3 s, the on-ramp CAV's target preceding vehicle is given CAV 4. The vehicle orders of other CAVs in each lane change accordingly when a CAV's desired vehicle sequence changes.

2) *Trajectories*: Fig. 6 and Fig. 7 show the acceleration and position trajectories in lane 1, lane 2, and lane 3, respectively, with the *first-in-first-out* method. Fig. 6(b) shows CAV 1's acceleration in lane 1 with black dashed line when CAVs in lane 2 and lane 1 affect each other to generate acceleration.

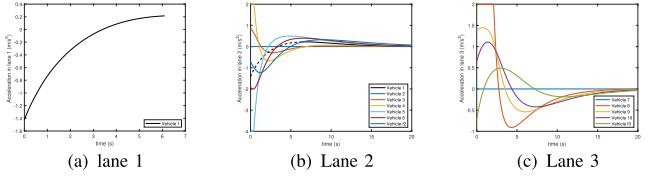


Fig. 6. Acceleration trajectories with the *first-in-first-out* method.

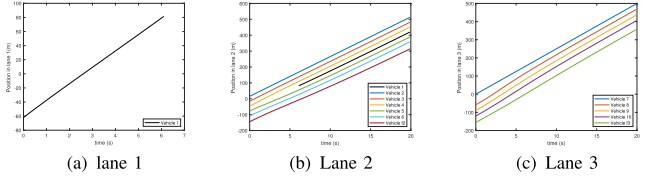


Fig. 7. Position trajectories with the *first-in-first-out* method.

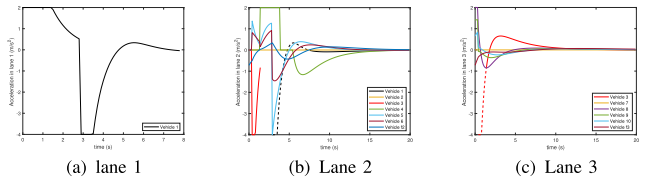


Fig. 8. Acceleration trajectories with the proposed hierarchical cooperative merging control approach.

Acceleration trajectories are reasonable based on the control objective of the operational controller with the *first-in-first-out* method. The *first-in-first-out* method assigns the on-ramp CAV to follow CAV 4 at 0 s. As a result, the initial gap errors for CAV 1 and 5 are negative. They decelerate and CAV 4 accelerates to reduce the gap errors. The deceleration of CAV 5 makes CAV 6's relative speed positive and gap error negative, and thus CAV 6 decelerate. Similarly, because the acceleration of CAV 4 makes its relative speed negative and gap error negative, CAV 3 accelerates. CAVs in lane 2 relax to equilibrium states respectively at around 20 s. At 5.2 s, CAV 1 is on the acceleration lane and has large enough inter-vehicle distances to CAV 4 and 5 respectively, and thus CAV 1 starts to turn left (See Fig. 7(b)). Initially, vehicle f2's actual gap equals its desired minimum gap and its speed is smaller than the speed limits. Based on (11), it decelerates. In lane 3, CAV 8 has a positive gap error at 0 s and thus it initially accelerates. This makes CAV 9's relative speed and gap error negative, and thus CAV 9 accelerates. Likewise, CAV 10 accelerates to reduce negative relative speed and gap error brought by CAV 9's acceleration. For the same reason as the vehicle f2's, vehicle f3 decelerates at 0 s.

Fig. 8 and Fig. 9 illustrate the acceleration and position trajectories with the proposed hierarchical cooperative merging control approach in lane 1, lane 2, and lane 3, respectively. To clearly show the interaction of CAVs from two different lanes during lane-changing processes, Fig. 8(b) uses the black dashed line to show corresponding CAV 1's acceleration trajectory in lane 1; Fig. 8(c) uses the red dashed line to show corresponding CAV 3's acceleration trajectory in lane 2.



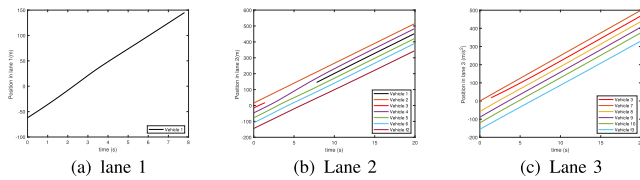


Fig. 9. Position trajectories with the proposed hierarchical cooperative merging control approach.

Fig. 8(b) shows three different obvious stages divided by 0.5 s, 1.5 s, and 3 s. At 0.5 s, CAV 3 is given CAV 7 as its desired directly preceding CAV. CAV 4 has a positive gap error and it is instructed to accelerate if the acceleration constraints are ignored. CAV 5 and CAV 6 accelerate accordingly to reduce gap errors and relative speeds caused by their directly preceding vehicles' acceleration, respectively. However, CAV 3 decelerates with  $-4 \text{ m/s}^2$ , CAV 4 is constrained to not accelerate, thus remaining  $0 \text{ m/s}^2$ . At 0.5 s, CAV 3 has large enough inter-vehicle distances to its surrounding vehicles and starts to turn left (See Fig. 9(b) and Fig. 9(c)). At 1.5 s, CAV 3 is in lane 3, it no longer affects CAV 4 and CAV 4 starts to accelerate to reduce its gap error. Before 3 s, the CAV 1 accelerates to reach the speed limits. At 3 s, the on-ramp CAV is given CAV 4 as its desired directly preceding vehicle. CAV 4 still has a positive gap error and it accelerates. CAV 1 has a negative gap error (See Fig. 9(b)) and a negative relative speed, and thus it decelerates. CAV 5 has a negative relative speed, and thus it decelerates. CAVs in lane 2 relax to their equilibrium states respectively at around 17 s, quicker than the situation with the *first-in-first-out* method. Vehicle f2 initially decelerates. It is affected by CAV 6, and thus its acceleration trajectory has three different turning points.

In lane 3, before 0.5 s, CAV 8 accelerates to reduce its positive gap error. CAV 9 and 10 accelerates as well to lessen their gap error and relative speed caused by their preceding vehicle's acceleration, respectively. At 0.5 s, CAV 3 has a negative gap error and decelerates. CAV 8 still has a positive gap error and accelerates (See Fig. 9(c) and Fig. 6(c)). CAVs in lane 3 relax to their equilibrium states respectively at around 15 s, quicker than the situation with the *first-in-first-out* method. Vehicle f3 decelerates at 0 s. Its acceleration trajectory has one turning point at 0.5 s.

3) *Performance Indicators*: The total disturbances for the upstream traffic during the simulation and the average speed of CAVs before leaving the end of the acceleration lane are selected as indicators. Their values are recorded to the nearest two decimal points. With the *first-in-first-out* method, the overall disturbances is  $10.40 \text{ m/s}^2$  and the average speed is  $25.03 \text{ m/s}$ . The average speed of f2 and vehicle f3 are  $23.01 \text{ m/s}$  and  $25.79 \text{ m/s}$ , respectively. The norm2 of their deceleration rates are  $5.81 \text{ m/s}^2$  and  $1.91 \text{ m/s}^2$ , respectively. The proposed hierarchical cooperative merging control approach brings  $6.45 \text{ m/s}^2$  and  $25.12 \text{ m/s}$ . The average speed of f2 and vehicle f3 are  $24.46 \text{ m/s}$  and  $24.33 \text{ m/s}$ , respectively. Their disturbances are  $2.36 \text{ m/s}^2$  and  $1.52 \text{ m/s}^2$ , respectively. By comparison, the hierarchical cooperative merging control approach reduces the disturbances by 37.94% and improves

average speed by 0.36%. The improvement is reflected by the average speeds and disturbances of vehicle f2 and vehicle f3 under the two different control approaches. With the proposed hierarchical cooperative merging control approach, a 49.74% reduction in the sum of disturbances of vehicle f2 and vehicle f3 is observed. Besides, the difference between the average speeds of vehicle f2 and vehicle f3 decreases.

#### D. Discussion

Simulation results show that the proposed hierarchical cooperative merging control approach outperforms the *first-in-first-out* method to reduce disturbances to upstream traffic (See Fig. 4). This implies that extra improvement in traffic operations can be achieved by exploring an optimal or a sub-optimal merging sequence.

By observation, the hierarchical cooperative merging control approach tends to make the on-ramp CAV (CAV 1) have a small vehicle order in lane 2 under equilibrium situations or when no mainline CAV is instructed to change lane and allows CAV 1 to accelerate for several seconds to get closer to downstream mainline CAVs in lane 2. The on-ramp CAV can reach the speed limits  $30 \text{ m/s}$  before it is given its desired future directly preceding vehicle or a merging sequence. Compared with the situations when a small gap exists in lane 3, the hierarchical cooperative merging control approach is more likely to instruct a mainline CAV close to the large gap in lane 2 to change lane when a large space exists in lane 3. Besides, the on-ramp CAV is given a new merging sequence no earlier than the mainline lane changer. The possibility that the on-ramp CAV utilizes the space generated by the mainline lane changer is high.

Under the 109 large gap scenarios and free flow scenarios where a mainline CAV is instructed to change lane by the hierarchical cooperative merging control approach, the on-ramp CAV 1 waits to change lane until the mainline lane changers have left lane 2 (See Fig. 5). However, under some scenarios, the CAV 1 does not directly use the gap created by the mainline lane changers to change lane. Compared with the choices of not allowing a mainline CAV to change lane, disturbances to upstream traffic decreases obviously (See Fig. 4). This implies that the existence of large gaps in lane 2 during on-ramp merging is helpful to reduce traffic disturbances. Assuming not taking other measures, if a mainline CAV's lane-changing behavior does not add much disturbances to lane 3, making it change lane may improve overall traffic operations during on-ramp merging.

The final vehicle sequences of mainline lane changers under small and large gap scenarios are 2 or 3 in lane 3 with the proposed hierarchical cooperative merging control approach. Because the small or large gaps locates before the initial second vehicle (vehicle 8) in lane 3, this finding suggests that the lane changers choose the small or large gap or the next upstream gap in lane 3 for lane changing.

Different choices of the last vehicles in lane 2 and lane 3 are possible based on different initial conditions. When no mainline vehicle changes lane, an on-ramp merging operation brings less traffic disturbances to upstream traffic if an on-ramp

vehicle accelerates to achieve a higher speed and has a smaller vehicle order in lane 2 after merging. This implies that the initial last vehicle in lane 2 can be the first upstream vehicle that is longitudinally behind the last upstream on-ramp vehicle if the on-ramp vehicle's speed is close to or higher than the speed of mainline traffic and the possibility of the existence of a mainline lane changer is low. If the speed of the on-ramp vehicle is lower, the initial last vehicle in lane 2 can be chosen based on predicted vehicular positions. To predict the future, the on-ramp vehicle may be assumed to accelerate with the maximum acceleration to reach the speed of mainline traffic; and mainline vehicles may be assumed to travel with constant speeds or update their accelerations by using a car-following model. When the on-ramp vehicle reaches the speed of mainline traffic based on the prediction, the first upstream vehicle in lane 2 that is longitudinally behind it can be chosen as the initial last vehicle. Besides, lane changers in lane 2 choose the slot between vehicle 7 and vehicle 8 or between vehicle 8 and vehicle 9 to change lane when a large or small gap exists between vehicle 7 and vehicle 8. This implies that the last vehicle in lane 3 can be the first following upstream vehicle of the vehicle that does not have desired inter-vehicle distance.

Optimal merging sequences are affected by both the planner's control objectives and the restrictions on mainline CAVs. The disturbances to upstream traffic are selected as a performance indicator to choose an optimal merging sequence by the planner. Besides, average speed, total travel time, control objectives of the operational controller, or time duration for on-ramp CAVs to accomplish merging can also be chosen as a performance indicator. The optimal merging sequences can be different accordingly [25]–[27], [29], [44], [50]. Distinguishing which performance indicators are critical in traffic management is an important research direction. When a mainline CAV is allowed to change lane, traffic operations can be further improved (See Fig. 4). Relaxing restriction on lane-changing maneuvers of mainline CAVs during merging is a promising research direction for efficient on-ramp merging in the future.

In subsection V-C, the hierarchical cooperative merging control approach reduces the disturbances by 37.94%. Surprisingly, the average speed is only improved by 0.36%. To this end, attenuating traffic disturbances during merging may not bring significant improvement in average speed.

CAVs in lane 2 may change lane to improve merging efficiency when a CAV's inter-vehicle distance is smaller than its desired value in lane 3 (See Fig. 4). Existing lane-changing models cannot cover this point. To this end, exploring new lane-changing models for CAVs that consider possible cooperation among CAVs is another promising research direction for merging.

By considering only one on-ramp CAV and assuming one mainline CAV may change lane to the left during merging, the possible combination of vehicle orders is countable and can be solved easily by enumeration. When more on-ramp CAVs are considered together and mainline CAVs are given more freedom to change lane, an effective solution for (5) is needed to enhance computation efficiency. A possible direction is to

express (5) with the initial states of vehicles and the planned dynamic vehicle sequences and to linearize the new expression by using approximation or conversion. Besides, the constraints should be converted into linear forms by conversion or adding logical variables. The optimization problem of the planner is then transformed into an integer linear programming problem which can be solved by using the existing integer programming algorithms.

Considering that mixed traffic of CAVs and human-driven vehicles is common for a long time, future studies should take into consideration mixed traffic. The proposed hierarchical cooperative merging control approach has the potential to be extended to include human-driven vehicles. The extension relies on the possibility to collect real-time accurate positions and speeds of the human-driven vehicles, to precisely describe the actual system behavior of vehicles, and to implement new traffic rules and regulations. The accurate information of human-driven vehicles can be obtained if they are equipped with V2V or V2I communication, or their directly following and preceding vehicles are CAVs. The description of the actual system behavior of vehicles includes the interaction between CAVs and human-driven vehicles. Because the motions of the human-driven vehicles can not be controlled, their behaviors may be affected by new traffic rules or regulations together with the behavior of surrounding CAVs. Besides, the extension also counts on developing efficient solution approaches for the corresponding optimization problems.

## VI. CONCLUSION AND OUTLOOK

The proposed hierarchical cooperative merging control approach has a maneuver planner and an operational trajectory controller which are formulated as model-based optimization, respectively. Importantly, the planner uses a linear prediction model to represent interactions among CAVs during merging. The planner, thus, can evaluate different dynamic vehicle sequences with a performance indicator (See (5)), and then establish optimal dynamic vehicle sequences in multiple lanes in a long time horizon. The operational controller regulates longitudinal acceleration trajectories and time instants for lane changers to change lane by utilizing model predictive control, subject to the admissible gap, speed, and acceleration constraints.

Fig. 4 has proved that the proposed hierarchical cooperative merging control approach outperforms the *first-in-first-out* method under 528 different initial settings including desired time gap, speed, and position of CAVs, bringing 11% to 91% reduction ratios in traffic disturbances.

Remarkably, the hierarchical control approach does not have restrictions on formulations of controllers, vehicle types, road layouts, or assumptions on lane-changing choices. To this end, it can be easily extended. To adapt to mixed traffic conditions, the hierarchical control approach can be further extended by including the interaction between automated vehicles and human-driven vehicles in the planner and operational controller, respectively. This will be addressed in our future research.

## REFERENCES

- [1] I. A. Ntousakis, I. K. Nikolos, and M. Papageorgiou, "Optimal vehicle trajectory planning in the context of cooperative merging on highways," *Transp. Res. C, Emerg. Technol.*, vol. 71, pp. 464–488, Oct. 2016.
- [2] B. van Arem, C. J. G. van Driel, and R. Visser, "The impact of cooperative adaptive cruise control on traffic-flow characteristics," *IEEE Trans. Intell. Transp. Syst.*, vol. 7, no. 4, pp. 429–436, Dec. 2006.
- [3] Y. Wang, E. Wenjuan, W. Tang, D. Tian, G. Lu, and G. Yu, "Automated on-ramp merging control algorithm based on internet-connected vehicles," *IET Intell. Transp. Syst.*, vol. 7, no. 4, pp. 371–379, 2013.
- [4] R. Pueboobpaphan, F. Liu, and B. van Arem, "The impacts of a communication based merging assistant on traffic flows of manual and equipped vehicles at an on-ramp using traffic flow simulation," in *Proc. 13th Int. IEEE Conf. Intell. Transp. Syst.*, Sep. 2010, pp. 1468–1473.
- [5] M. Zhou, X. Qu, and S. Jin, "On the impact of cooperative autonomous vehicles in improving freeway merging: A modified intelligent driver model-based approach," *IEEE Trans. Intell. Transp. Syst.*, vol. 18, no. 6, pp. 1422–1428, Jun. 2017.
- [6] L.-Y. Xiao and F. Gao, "Effect of information delay on string stability of platoon of automated vehicles under typical information frameworks," *J. Central South Univ. Technol.*, vol. 17, no. 6, pp. 1271–1278, Dec. 2010.
- [7] S. Shladover, D. Su, and X.-Y. Lu, "Impacts of cooperative adaptive cruise control on freeway traffic flow," *Transp. Res. Rec., J. Transp. Res. Board*, vol. 2324, pp. 63–70, Dec. 2012.
- [8] J. Rios-Torres and A. A. Malikopoulos, "A survey on the coordination of connected and automated vehicles at intersections and merging at highway on-ramps," *IEEE Trans. Intell. Transp. Syst.*, vol. 18, no. 5, pp. 1066–1077, May 2017.
- [9] N. Chen, M. Wang, T. Alkim, and B. van Arem, "A robust longitudinal control strategy of platoons under model uncertainties and time delays," *J. Adv. Transp.*, vol. 2018, Apr. 2018, Art. no. 9852721.
- [10] N. Chen, M. Wang, T. Alkim, and B. Van Arem, "A flexible strategy for efficient merging maneuvers of connected automated vehicles," in *Proc. CICTP*, Jul. 2018, pp. 46–55.
- [11] W. Zhao, R. Liu, and D. Ngduy, "A bilevel programming model for autonomous intersection control and trajectory planning," *Transportmetrica A, Transp. Sci.*, vol. 17, no. 1, pp. 34–58, 2019.
- [12] G. Schmidt and B. Posch, "A two-layer control scheme for merging of automated vehicles," in *Proc. 22nd IEEE Conf. Decis. Control*, Dec. 1983, pp. 495–500.
- [13] V. Milanés, J. Godoy, J. Villagrà, and J. Pérez, "Automated on-ramp merging system for congested traffic situations," *IEEE Trans. Intell. Transp. Syst.*, vol. 12, no. 2, pp. 500–508, Jun. 2011.
- [14] J. Guanetti, Y. Kim, and F. Borrelli, "Control of connected and automated vehicles: State of the art and future challenges," *Annu. Rev. Control*, vol. 45, pp. 18–40, May 2018.
- [15] M. Bahram, C. Hubmann, A. Lawitzky, M. Aeberhard, and D. Wollherr, "A combined model-and learning-based framework for interaction-aware Maneuver prediction," *IEEE Trans. Intell. Transp. Syst.*, vol. 17, no. 6, pp. 1538–1550, Jun. 2016.
- [16] N. Evestedt, E. Ward, J. Folkesson, and D. Axehill, "Interaction aware trajectory planning for merge scenarios in congested traffic situations," in *Proc. IEEE 19th Int. Conf. Intell. Transp. Syst. (ITSC)*, Nov. 2016, pp. 465–472.
- [17] R. Scarinci, B. Heydecker, and A. Hegyi, "Analysis of traffic performance of a merging assistant strategy using cooperative vehicles," *IEEE Trans. Intell. Transp. Syst.*, vol. 16, no. 4, pp. 2094–2103, Aug. 2015.
- [18] R. W. Hall and H.-S. J. Tsao, "Capacity of automated highway systems: Merging efficiency," in *Proc. Amer. Control Conf.*, vol. 3, Jun. 1997, pp. 2046–2050.
- [19] B. Posch and G. Schmidt, "A comprehensive control concept for merging of automated vehicles under a broad class of traffic conditions," *IFAC Proc. Volumes*, vol. 16, no. 4, pp. 187–194, Apr. 1983.
- [20] W. Cao, M. Mukai, T. Kawabe, H. Nishira, and N. Fujiki, "Cooperative vehicle path generation during merging using model predictive control with real-time optimization," *Control Eng. Pract.*, vol. 34, pp. 98–105, Jan. 2015.
- [21] R. Scarinci and B. Heydecker, "Control concepts for facilitating motorway on-ramp merging using intelligent vehicles," *Transp. Rev.*, vol. 34, no. 6, pp. 775–797, 2014.
- [22] J. Rios-Torres and A. A. Malikopoulos, "Automated and cooperative vehicle merging at highway on-ramps," *IEEE Trans. Intell. Transp. Syst.*, vol. 18, no. 4, pp. 780–789, Apr. 2017.
- [23] Y. Xie, H. Zhang, N. H. Gartner, and T. Arsava, "Collaborative merging strategy for freeway ramp operations in a connected and autonomous vehicles environment," *J. Intell. Transp. Syst.*, vol. 21, no. 2, pp. 136–147, 2017.
- [24] Y. Zhou, E. Chung, A. Bhaska, and M. E. Cholette, "A state-constrained optimal control based trajectory planning strategy for cooperative freeway mainline facilitating and on-ramp merging maneuvers under congested traffic," *Transp. Res. C, Emerg. Technol.*, vol. 109, pp. 321–342, Dec. 2019.
- [25] M. Athans, "A unified approach to the vehicle-merging problem," *Transp. Res.*, vol. 3, no. 1, pp. 123–133, Apr. 1969.
- [26] T. Awal, L. Kulik, and K. Ramamohanrao, "Optimal traffic merging strategy for communication-and sensor-enabled vehicles," in *Proc. 16th Int. IEEE Conf. Intell. Transp. Syst. (ITSC)*, Oct. 2013, pp. 1468–1474.
- [27] N. Chen, B. van Arem, T. Alkim, and M. Wang, "A hierarchical model-based optimization control approach for cooperative merging by connected automated vehicles," *IEEE Trans. Intell. Transp. Syst.*, vol. 22, no. 12, pp. 7712–7725, Dec. 2021, doi: [10.1109/TITS.2020.3007647](https://doi.org/10.1109/TITS.2020.3007647).
- [28] J. Ding, L. Li, H. Peng, and Y. Zhang, "A rule-based cooperative merging strategy for connected and automated vehicles," *IEEE Trans. Intell. Transp. Syst.*, vol. 21, no. 8, pp. 3436–3446, Aug. 2020.
- [29] A. Duret, M. Wang, and A. Ladino, "A hierarchical approach for splitting truck platoons near network discontinuities," *Transp. Res. Proc.*, vol. 38, pp. 627–646, Jan. 2019.
- [30] H. Min, Y. Fang, R. Wang, X. Li, Z. Xu, and X. Zhao, "A novel on-ramp merging strategy for connected and automated vehicles based on game theory," *J. Adv. Transp.*, vol. 2020, Jul. 2020, Art. no. 2529856.
- [31] C. Roncoli, I. Papamichail, and M. Papageorgiou, "Hierarchical model predictive control for multi-lane motorways in presence of vehicle automation and communication systems," *Transp. Res. C, Emerg. Technol.*, vol. 62, pp. 117–132, Jan. 2016.
- [32] Z. Sun, T. Huang, and P. Zhang, "Cooperative decision-making for mixed traffic: A ramp merging example," *Transp. Res. C, Emerg. Technol.*, vol. 120, Nov. 2020, Art. no. 102764.
- [33] H. Li, J. Zhang, Z. Zhang, and Z. Huang, "Active lane management for intelligent connected vehicles in weaving areas of urban expressway," *J. Intell. Connected Vehicles*, vol. 4, no. 2, pp. 52–67, Sep. 2021.
- [34] Y. Ali, Z. Zheng, and M. M. Haque, "Modelling lane-changing execution behaviour in a connected environment: A grouped random parameters with heterogeneity-in-means approach," *Commun. Transp. Res.*, vol. 1, Dec. 2021, Art. no. 100009.
- [35] J. Larsson, M. F. Keskin, B. Peng, B. Kulcsár, and H. Wymeersch, "Pro-social control of connected automated vehicles in mixed-autonomy multi-lane highway traffic," *Commun. Transp. Res.*, vol. 1, Dec. 2021, Art. no. 100019.
- [36] C. Li, Y. Xie, G. Wang, X. Zeng, and H. Jing, "Lateral stability regulation of intelligent electric vehicle based on model predictive control," *J. Intell. Connected Vehicles*, vol. 4, no. 3, pp. 104–114, Dec. 2021.
- [37] J. Nilsson, J. Silvlin, M. Brannstrom, E. Coelingh, and J. Fredriksson, "If, when, and how to perform lane change maneuvers on highways," *IEEE Intell. Transp. Syst. Mag.*, vol. 8, no. 4, pp. 68–78, Oct. 2016.
- [38] L. Xiao, M. Wang, W. Schakel, and B. van Arem, "Unravelling effects of cooperative adaptive cruise control deactivation on traffic flow characteristics at merging bottlenecks," *Transp. Res. C, Emerg. Technol.*, vol. 96, pp. 380–397, Nov. 2018.
- [39] T.-S. Dao, J. P. Huissoon, and C. M. Clark, "A strategy for optimisation of cooperative platoon formation," *Int. J. Vehicle Inf. Commun. Syst.*, vol. 3, no. 1, pp. 28–43, 2013.
- [40] S. Karbalaieali, O. A. Osman, and S. Ishak, "A dynamic adaptive algorithm for merging into platoons in connected automated environments," *IEEE Trans. Intell. Transp. Syst.*, vol. 21, no. 10, pp. 4111–4122, Oct. 2020.
- [41] X. Hu and J. Sun, "Trajectory optimization of connected and autonomous vehicles at a multilane freeway merging area," *Transp. Res. C, Emerg. Technol.*, vol. 101, pp. 111–125, Apr. 2019.
- [42] H. Xu, Y. Zhang, C. G. Cassandras, L. Li, and S. Feng, "A bi-level cooperative driving strategy allowing lane changes," *Transp. Res. C, Emerg. Technol.*, vol. 120, Nov. 2020, Art. no. 102773.
- [43] P. Hang, C. Lv, C. Huang, Y. Xing, and Z. Hu, "Cooperative decision making of connected automated vehicles at multi-lane merging zone: A coalitional game approach," *IEEE Trans. Intell. Transp. Syst.*, vol. 23, no. 4, pp. 3829–3841, Apr. 2022, doi: [10.1109/TITS.2021.3069463](https://doi.org/10.1109/TITS.2021.3069463).
- [44] H. Ding, Y. Di, X. Zheng, H. Bai, and W. Zhang, "Automated cooperative control of multilane freeway merging areas in connected and autonomous vehicle environments," *Transportmetrica B, Transp. Dyn.*, vol. 9, no. 1, pp. 437–455, Jan. 2021.



- [45] C. F. Daganzo, M. J. Cassidy, and R. L. Bertini, "Possible explanations of phase transitions in highway traffic," *Transp. Res. A, Policy Pract.*, vol. 33, no. 5, pp. 365–379, 1999.
- [46] S. Feng, Y. Zhang, S. E. Li, Z. Cao, H. X. Liu, and L. Li, "String stability for vehicular platoon control: Definitions and analysis methods," *Annu. Rev. Control*, vol. 47, pp. 81–97, Mar. 2019.
- [47] S. Samiee, S. Azadi, R. Kazemi, and A. Eichberger, "Towards a decision-making algorithm for automatic lane change manoeuvre considering traffic dynamics," *PROMET-Traffic Transp.*, vol. 28, no. 2, pp. 91–103, Apr. 2016.
- [48] M. Wang, S. P. Hoogendoorn, W. Daamen, B. van Arem, and R. Happee, "Game theoretic approach for predictive lane-changing and car-following control," *Transp. Res. C, Emerg. Technol.*, vol. 58, pp. 73–92, Sep. 2015.
- [49] A. Kesting, M. Treiber, and D. Helbing, "General lane-changing model MOBIL for car-following models," *Transp. Res. Rec.*, vol. 1999, no. 1, pp. 86–94, Jan. 2007.
- [50] N. Chen, B. V. Arem, and M. Wang, "Optimization of traffic efficiency at on-ramps with connected automated vehicles," in *Proc. Forum Integr. Sustain. Transp. Syst. (FISTS)*, Nov. 2020, pp. 230–235.



**Na Chen** received the B.Eng. degree in traffic and transportation and the M.Eng. degree in traffic and transportation planning and management from Beijing Jiaotong University, Beijing, China, in 2013 and 2016, respectively, and the Ph.D. degree in traffic information engineering and control from the Delft University of Technology, the Netherlands, in 2021. Her research interests include intelligent vehicle systems, intelligent traffic systems, driver behavior, traffic safety, and traffic management.



**Bart van Arem** (Senior Member, IEEE) received the M.Sc. and Ph.D. degrees in applied mathematics from the University of Twente, Enschede, the Netherlands, in 1986 and 1990, respectively. From 1992 to 2009, he was a Researcher and a Program Manager at TNO, working on intelligent transport systems, in which he has been active in various national and international projects. From 2009 to 2018, he was the Chair Professor of transport modeling at the Department of Transport and Planning, Delft University of Technology, the Netherlands, where he is a Full-Time Professor, focusing on the impact of intelligent transport systems on mobility. His research interests include transport modeling and intelligent vehicle systems.



**Meng Wang** (Member, IEEE) received the B.Sc. degree from Tsinghua University in 2003, the M.Sc. degree from the Research Institute of Highway (RIOH), Ministry of Transport, in 2006, and the Ph.D. degree (Hons.) from TU Delft in 2014. He was an Assistant Professor (tenured in 2019) at the Department of Transport and Planning of TU Delft, from 2015 to 2021 and the Co-Director of the Electric and Automated Transport Laboratory (hEAT lab). From 2006 to 2009, he was an Assistant Researcher at the National ITS Center of RIOH and a Post-Doctoral Researcher at the Automotive Group, Faculty of Mechanical Engineering, TU Delft, from 2014 and 2015. He is a Full Professor (W3) and the Head of the Chair of Traffic Process Automation with the "Friedrich List" Faculty of Transport and Traffic Sciences, Technische Universität Dresden. His main research interests are traffic flow modelling and control, driver behaviour, control design, and impact assessment of connected and automated vehicles. He was a recipient of the IEEE ITS Society Best Ph.D. Dissertation Award in 2015 and the IEEE International Conference on Intelligent Transportation Systems (ITSC) Best Paper Award in 2013. He is an Associate Editor of the journal IEEE TRANSACTIONS ON INTELLIGENT TRANSPORTATION SYSTEMS, IET ITS, and *Transportmetrica B* and the Editorial Board Member of *Transportation Research Part C*.